Extremal Dependence between Temperature and Ozone over the Continental U.S.

Pakawat Phalitnonkiat[1], Wenxiu Sun[2], Mircea D. Grigoriu[3], Peter G. M. Hess[4],
Gennady Samorodnitsky[5], and Simone Tilmes[6]

[1]Center for Applied Math, Cornell University
[2]Department of Biological and Environmental Engineering, Cornell University
[3]School of Civil and Environmental Engineering, Cornell University
[4]Department of Biological and Environmental Engineering, Cornell University
[5]School of Operations Research and Information Engineering, Cornell University
[6]Atmospheric Chemistry Observations & Modeling Laboratory

Correspondence to: Peter G. M. Hess (pgh25@cornell.edu)

Abstract. The co-occurrence of heat waves and pollution events and the resulting high mortality rates emphasizes the importance of the co-occurrence of pollution and temperature extremes. Through the use of extreme value theory and other statistical methods ozone and temperature extremes and their joint occurrence are analyzed over the United States during the summer months (JJA) using Clean Air Status and Trends Network (CASTNET) measurement data and simulations of the present

5 and future climate and chemistry in the Community Earth System Model (CESM1) CAM4-chem. Three simulations using CAM4-chem were analyzed: the Chemistry Climate Model Initiative (CCMI) reference experiment using specified dynamics (REFC1SD) between 1992-2010, a 25-year present-day simulation branched off the CCMI REFC2 simulation in the year 2000 and a 25-year future simulation branched off the CCMI REFC2 simulation in 2100. The latter two simulations differed in their concentration of carbon dioxide (representative of the years 2000 and 2100) but were otherwise identical. A new metric is

10 developed to measure the joint extremal dependence of ozone and temperature by evaluating the spectral dependence of their extremes. Two regions of the U.S. give the strongest measured extreme dependence of ozone and temperature: the northeast and the southeast. The simulations do not capture the relationship between temperature and ozone over the northeast but do simulate a strong dependence of ozone on extreme temperatures over the southeast. In general, the simulations of ozone and temperature do not capture the width of the measured temperature and ozone distributions. While on average the future increase

15 in the 90th percentile temperature and the 90th percentile ozone slightly exceed the mean increase over the continental U.S., in many regions the width of the temperature and ozone distributions decrease. The location of future increases in the tails of the ozone distribution are weakly related to those of temperature with a correlation of 0.3.

Atmospheric
Chemistry
and Physics
Discussions

1 Introduction

The climate change ozone penalty refers to the additional emission cuts needed to meet regulatory ozone limits in the face of climate change (Wu et al. (2008)). Increases in future pollutant levels have been attributed to higher temperatures, more frequent and longer duration of stagnation events, and decreases in the frequency of frontal passages (e.g., Fiore et al. (2015)).

5 The European heat wave of 2003, the Russian heat wave of 2010 and the extreme pollution that accompanied both events underline the dangers of a future increase in heat waves and the accompanying air pollution. It has been estimated that more people will die due to outdoor air quality in 2030 rather than any other environmental factors (OECD (2012)).

Summertime increases in temperature over the U.S. are expected in the next century in all climate scenarios (Collins et al. (2013)). Porter et al. (2015) found that over most of the U.S. temperature is the first meteorological covariate with ozone.

10 Ozone concentrations increase with temperature due to temperature related photochemistry, but also due to the meteorological and emission changes that correlate with temperature (e.g., see Fiore et al. (2015)). Increases in ozone with temperature have been reported in the range from 2-8 ppbv $°C^{-1}$ depending on details of the analysis (Brown-Steiner et al. (2015)). The relation between ozone and temperature is complex: it is determined by the impact of meteorological factors which impact ozone such as stagnation events or cloud cover (e.g., see Jacob and Winner,2009), by temperature dependent ozone chemistry (Pusede et al.

15 (2015)) and by temperature dependent emissions(e.g., Weaver et al. (2009)). While the ozone-temperature relationship is often measured with a linear slope (e.g., Steiner et al. (2010)), when it comes to extreme values, the relationship between temperature and ozone becomes more complicated (e.g., Steiner et al. (2010), Shen et al. (2016)). Here we examine the relationship between temperature extremes and ozone extremes in measurements and in current and future model simulations. An analysis of the extremes in ozone and temperature together may be particularly important as their joint impact on mortality is likely nonlinear

20 (Wilson et al. (2014), Dear et al. (2005), Ren et al. (2008)).

The future relation between ozone extremes and temperature extremes depends on i) the nature of future temperature extremes and ii) the impact of these extremes on ozone. Globally the increase in the 20-year return period of high temperatures over land in CMIP5 is similar to the increase in mean temperature (Seneviratne et al. (2012)), although there are some important regional exceptions. This would suggest that for the most part, the future temperature probability distribution simply shifts to higher temperatures but does not change in shape consistent with measured trends (McKinnon et al. (2016)). On the other

25 hand, many studies suggest that the ozone distribution will increase predominantly on the high-end due to changes in climate (e.g., see Weaver et al. (2009)) although not all (e.g., Rieder et al. (2015)). At high enough temperatures (>312 K), Steiner et al. (2010) finds that the ozone increase with temperature is suppressed. Steiner et al. (2010) hypothesizes that this is due to the diminished role of PAN chemistry and isoprene emissions at high temperatures. Shen et al. (2016) shows that ozone suppression

30 at high temperature occurs at 23% of the CASTNET sites but hypothesize that the suppression is meteorologically induced. Based on the statistical relationship between ozone and temperature in the present climate, Shen et al. (2016) predicts that future temperatures will lead to an average increase of 2.6 ozone violations per year in 2060 across the US. Here we analyze the relationship between temperature and ozone extremes in measurements and in simulated present and future climates.

This article is organized as follows: in Sect. 2, we describe the datasets and model simulations used; in Sect. 3, we introduce the statistical procedures used to quantify the relationship between ozone and temperature. In Sect. 4, we present the results then discuss these results in Sect. 5, and Sect. 6 gives the conclusions.

2 Data and model descriptions

In this study we examine the relationship between ozone extremes in three model simulations over the U.S. as well as in the ozone and temperature measurements at 25 selected sites from the clean air status and trends network (CASTNET: www.epa.gov/castnet) from 1992-2010 (see Fig. 2 for station locations). CASTNET sites are situated to sample regional ozone concentrations so as to minimize the more local impact of urban areas.

The chemical emissions and forcing data for the model simulations are given in Table 1. The REFC1SD simulation (see Tilmes et al. (2016)) uses analyzed meteorological data from MERRA from 1992-2010 and time changing anthropogenic and biomass burning emissions as specified in Table 1. The other two model simulations, GCM2000 and GCM2100 are run as general circulation models so that the meteorology, sea surface temperatures (SST) and sea-ice are calculated internally. The GCM2000 and GCM2100 are 25-year simulations branched off the chemistry-climate model initiative (CCMI) REFC2 (Tilmes et al. (2016)) simulations in the year 2000 and the year 2100, respectively. The first five years of each simulation are considered as spin-up part with the latter 20 years analyzed in this study (2006-2025 for GCM2000 and 2106-2125 for GCM2100). Note that while the CO2 concentration in GCM2000 and GCM2100 represent the CO2 concentrations for the year 2000 and 2100, the concentrations of all other greenhouse gases including methane are fixed at their year 2000 concentrations. Note also that the emissions of chemical species, including biogenic emissions, in the GCM2000 and GCM2100 simulations are the same and remain fixed at the year 2000. The global mean temperature change over the continental US. between GCM2000 and GCM2100 is $2.1°C$, while the temperature difference in the parent CCMI REFC2 simulations following the representation concentration pathway 6 (RCP6) is $2.8°C$. The smaller temperature increase from GCM2000 to GCM2100 is likely due to the fact that the emissions of GHGs and short-lived forcing agents are held constant at the year 2000 levels in both simulations. In particular the aerosol emissions remain the same.

Detailed descriptions of CESM with chemistry are given in Lamarque et al. (2012). Brown-Steiner et al. (2015) has evaluated both the specified dynamics and free-running model configurations against measurements over the U.S., including comparisons of their respective ozone return periods. The horizontal grid resolution in all simulations is $1.9° \times 2.5°$; the CGM 2000 and GCM2100 simulations both have 26 vertical levels while the REFC1SD simulation has 56 vertical levels.

U.S. summertime ozone and temperature data (1 June to 30 August) are analyzed from both CASTNET and the three model simulations over the U.S. Ozone data is used from the first model level which provides a good estimate of the 10-meter ozone concentrations as measured by CASTNET (Brown-Steiner et al. (2015)). In both CASTNET and the model data, the maximum daily 8-hour average ozone concentrations (MDA8) are used. The maximum daily 2-meter temperature is also used in both the measurements and the simulations.

To render the data approximately stationary on both the interannual and seasonal basis, we adopt the procedures used in Phalitnonkiat et al. (2016). Formally, let $x_{y,d}$ represent the data on day d in year y, where x refers to either daily maximum temperature or MDA8 ozone. Since there are 91 days included in each summer period and 20 years (19 years for REFC1SD), $d = 1$ refers to 1 June and $d = 91$ refers to 30 August.

5   To minimize year-to-year variability so as to minimize any ozone trends while still keeping extreme data relevant, for each year y, we take the average of the data over that year but omit a number (a) of the highest values. That is, for a fixed year y, the resulting average is $m_{y,a}$:

$$m_{y,a} := \frac{1}{D-a} \sum_{i=1}^{D-a} x_{y,(i)} \tag{1}$$

where $D = 91$ is the total number of days for each year, and $x_{y,(i)}$ is the order statistic of the fixed year y: $x_{y,(1)} \leq x_{y,(2)} \leq \dots \leq x_{y,(D)}$. Then, we calculate a daily ozone deviation:

$$\hat{x}_{y,d}^{G} = x_{y,d} - m_{y,a}. \tag{2}$$

10   In our analysis, we use $a = 10$ as the default value which preserves about 11% of the extreme data. To eliminate seasonal effects, we average $\hat{x}_{y,d}^{G}$ for each day d over all years $Y = 20$ (or $Y = 19$ for REFC1SD). That is, for each day d, we calculate:

$$M_d = \frac{1}{Y} \sum_{y=1}^{Y} \hat{x}_{y,d}^{G}. \tag{3}$$

M_d is then smoothed by local polynomial regression since our sample size is rather small. In order not to overburden the notation, we will still use the notation M_d for the smoothed values of the estimates. Then we normalize the data by

$$\hat{x}_{y,d}^{DS} = \frac{\hat{x}_{y,d}^{G} - M_d}{sd_d}, \tag{4}$$

where $sd_d = \sqrt{\frac{1}{Y} \sum_{y=1}^{Y} (\hat{x}_{y,d}^{G} - M_d)^2}$ is the standard deviation of day d. Later in the text, we refer to (4) as a normalized scale.

15   In addition to the transformations from Phalitnonkiat et al. (2016), we add another procedure to revert the normalized scale data back to its original scale while keeping the stationarity. That is, we rescale $\hat{x}_{y,d}^{DS}$ back to its original scale ($\hat{x}_{y,d}^{res}$) by using the formula:

$$\hat{x}_{y,d}^{res} = \hat{x}_{y,d}^{DS} \times \left(\frac{1}{D} \sum_{d'=1}^{D} sd_{d'} \right) + \frac{1}{D} \sum_{d'=1}^{D} M_{d'} + \frac{1}{Y} \sum_{y'=1}^{Y} m_{y',a}, \tag{5}$$

where $Y = 20$ (or $Y = 19$ for REFC1SD).

3   Methodology

20   In this study besides using conventional methods, such as correlations, to quantify the relationship between temperature and ozone we also propose a novel metric to capture the relationship between ozone and temperature extremes. Correlation coefficients are inadequate for capturing the relationship between the extremes of two variables since they are estimated from all

Atmospheric
Chemistry
and Physics
Discussions

observations and extremes represent a small percentage of these observations. An alternative metric is proposed using only the largest values of two variables. After some transformations which act to normalize the two variables (see Appendix B), their extreme dependency is characterized by a probability density function (pdf) that measures the angular density when the variables are plotted against each other. The area under the pdf is 1 by definition and the range of the pdf is $\left[0, \frac{\pi}{2}\right]$. If the mass

5 of the pdf is concentrated near 0 or near $\frac{\pi}{2}$, extremes of the two variables are unlikely to be significant at the same time, which points to an independence of the extremes. On the other hand, if the mass of the pdf is concentrated away from the endpoints $0, \frac{\pi}{2}$, then simultaneous extremes of the two variables are likely. We refer to the procedure which normalizes the tails of the data so that the method described above works *the ranks method* (see Appendix B).

Since the area under the curve from 0 to $\pi/2$ is 1, we can consider only the area of the 'middle' part, which we define to be

10 between $\frac{\pi}{8}$ and $\frac{3\pi}{8}$, to represent the extreme dependence between two variables. Denote this amount by φ:

$$\varphi := \text{area} \left[\frac{\pi}{8}, \frac{3\pi}{8}\right]. \tag{6}$$

See the detailed explanation in C. Note that the range of φ is $[0, 1]$, where $\varphi = 1$ refers to extreme dependence and extreme independence implies $\varphi = 0$.

Figure 1 shows different scenarios of correlation and extreme dependence. Figure 1a gives a scenario of data with high correlation, yet the extremes of the data are only moderately dependent (Fig. 1c). In contrast, Fig. 1b gives an example of data

15 with low correlation but highly dependent extremes (Fig. 1d).

4   Results

In this section we compare measured and simulated temperature and ozone records separately (Sect. 4.1) and then their joint dependence are analyzed in Sect. 4.2. The extremes of ozone and temperature and their extremal dependence is emphasized. Simulated ozone and temperature records are from the REFC1SD, GCM2000 and GCM2100 simulations. In the REFC1SD

20 and GCM2000 simulations, we emphasize a comparison with the measured temperature and ozone records from CASTNET. For any given simulation, all percentiles are given with respect to that particular simulation. In particular, percentiles for the future simulations are given in terms of the future distributions.

4.1   Separate evaluation of temperature and ozone

The highest rescaled average temperatures naturally occur in the South with local maximum in the southwestern US, the

25 midwestern region and the east coast (Fig. 2a, c, e). The simulations do not represent the topography with the accuracy adequate to simulate temperatures in regions of large topographic relief characteristic of the western US. Overall, when evaluated at the CASTNET sites, temperature is slightly underestimated in the REFC1SD simulations and slightly overestimated in the GCM2000 simulations (see Table 2). The spatial correlation between measured and simulated rescaled temperature in the REFC1SD and GCM2000 simulation is between 0.57 and 0.53 respectively. In the GCM2100 simulation, rescaled temperature

30 increases by $2.43°C$ on average over the US compared with the GCM2000 simulation (Fig. 2c, e and Table 2), where the

Atmospheric
Chemistry
and Physics
Discussions

(a) Correlation = 0.7

(b) Correlation = -0.05

(c) Estimated spectral density = 0.22

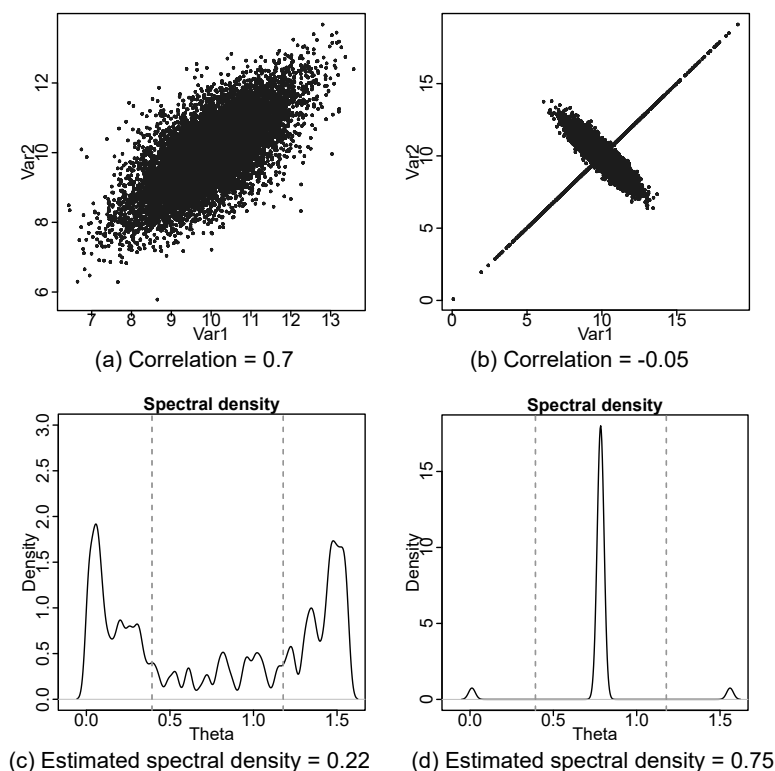(d) Estimated spectral density = 0.75

Figure 1. Examples that shows the correlation and extremal measure of dependence between two variables are not necessarily the same. The plots on the left column (a,c) use the data generated by Gaussian random vectors with correlation $\rho = 0.7$ and each component has $n = 10000$ points sampled from $N(10, 1)$, where $N(\mu, \sigma^2)$ is the normal distribution with mean μ and variance σ^2. The data are moderately correlated, while it has low extreme dependence (true $\varphi = 0$; estimated $\varphi = 0.223$). The plots on the right column (b,d) use the data generated by $(Var_1, Var_2) = (Y_1, Y_2)$ with probability 0.8 and $(Var_1, Var_2) = (Z, Z)$ with probability 0.2, where $(Y_1, Y_2) \sim N\left(\mu = [10, 10]^T, \Sigma = [1, -0.9; -0.9, 1]\right)$ follows a bivariate normal, where μ is the mean vector and Σ is the covariance matrix, and $Z \sim N(\mu = 10, \sigma^2 = 9)$. The sample size is also $n = 10000$. The plots show the existence of tail dependence by having high angular density near $\frac{\pi}{4}$ ($\varphi = 0.75$); however, low correlation (true $\rho = 0$; estimated $\rho = -0.05$).

Atmospheric
Chemistry
and Physics
Discussions

regions of high temperatures in the GCM2100 simulation expand prominently with a tongue of high temperatures extending throughout the midwest. In contrast, the width of the high-end temperature distribution which can be calculated by difference between the 90th percentile and average temperatures (i.e., $mean(T|T > 90\%) - mean(T)$) maximizes in the northern part of the domain, but with a tongue of high temperatures differences extending southwards through the midwest (Fig. 2b, d, f).

5　Both the REFC1SD and GCM2000 simulations underestimate $mean(T|T > 90\%) - mean(T)$. There is some evidence of this pattern in the CASTNET measurements. Overall, the conditional temperature differences show little response to climate change (e.g., compare Fig. 2d and 2f) suggesting the high end of the future temperature distribution does change markedly with respect to the mean. This is consistent with the historical changes in the temperature distributions (McKinnon et al. (2016), Rhines and Huybers (2013)).

10　In all simulations rescaled ozone is highest in the southwestern US and in the middle Atlantic regions extending towards the central midwest (Fig. 3a, c, e). This westward extent of this ozone maximum is not reflected in the CASTNET data. Consistent with many GCMs (e.g., Lamarque et al. (2012); Rieder et al. (2015)), the REFC1SD and GCM simulations have the highest surface ozone biases in the Northeast with the smallest biases in the Southeast (Table 2). Averaged over all CASTNET stations simulated surface ozone is biased high by approximately 12 ppb in the REFC1SD simulations and 21 ppb in the GCM2000

15　simulation. The spatial correlation between measured and simulated ozone in the REFC1SD simulation and GCM2000 simulation are 0.24 and 0.23 respectively (with p-value at 0.25 and 0.26, respectively for the alternative hypothesis of the correlation not being 0). In the GCM2100 simulation, ozone increases by approximately 3 ppb averaged over the US with respect to the GCM2000 simulation (Fig. 3e and Table 2).

The simulated difference between the 90th percentile and average ozone is biased low (Fig. 3b, d) with average biases of

20　-0.79 and -4.28 ppb in the REFC1SD and GCM2000 simulations, respectively. However, the overall simulated pattern is similar to the measurements with the largest differences in the eastern part of the domain.

The geographic pattern for the high-end width of the ozone distribution ($mean(O3|O3 > 90\%) - mean(O3)$) is significantly different from the equivalent quantity for temperature. While the width of the temperature distribution ($mean(T|T > 90\%) - mean(T)$) maximizes in the central US (Fig. 2b, d, f) while the width of the ozone distribution maximizes in the eastern US

25　(Fig. 3b, d, f). On average the difference between the 90th percentile ozone and average ozone increases only by 0.26 ppb in the future simulation (Fig. 3f).

The relative difference between changes in extreme values and the change in median values in a future simulation compared to the present day simulation can be expressed as the quantity Ψ.

$$\Psi(X,Y) := \frac{\text{Mean\_GCM2100}(X|Y > 90\%) - \text{Mean\_GCM2100}(X|45\% < Y < 55\%)}{\text{Mean\_GCM2000}(X|Y > 90\%) - \text{Mean\_GCM2000}(X|45\% < Y < 55\%)}, \tag{7}$$

where X, Y are ozone or temperature. If the change in extreme increments in X given Y in the GCM2100 and GCM2000

30　simulations are the same, we expect the ratio to be 1.

The high-end width of the future temperature distribution is projected to increase relative to the present day temperature distribution by up to 30% in the Southeast US extending Northwards through the eastern midwest (see Fig. 4b). In contrast, $\Psi(O_3, O_3)$ is less than 1 over much of the domain (Fig. 4a). Note, however, that the region where $\Psi(O_3, O_3)$ is slightly greater
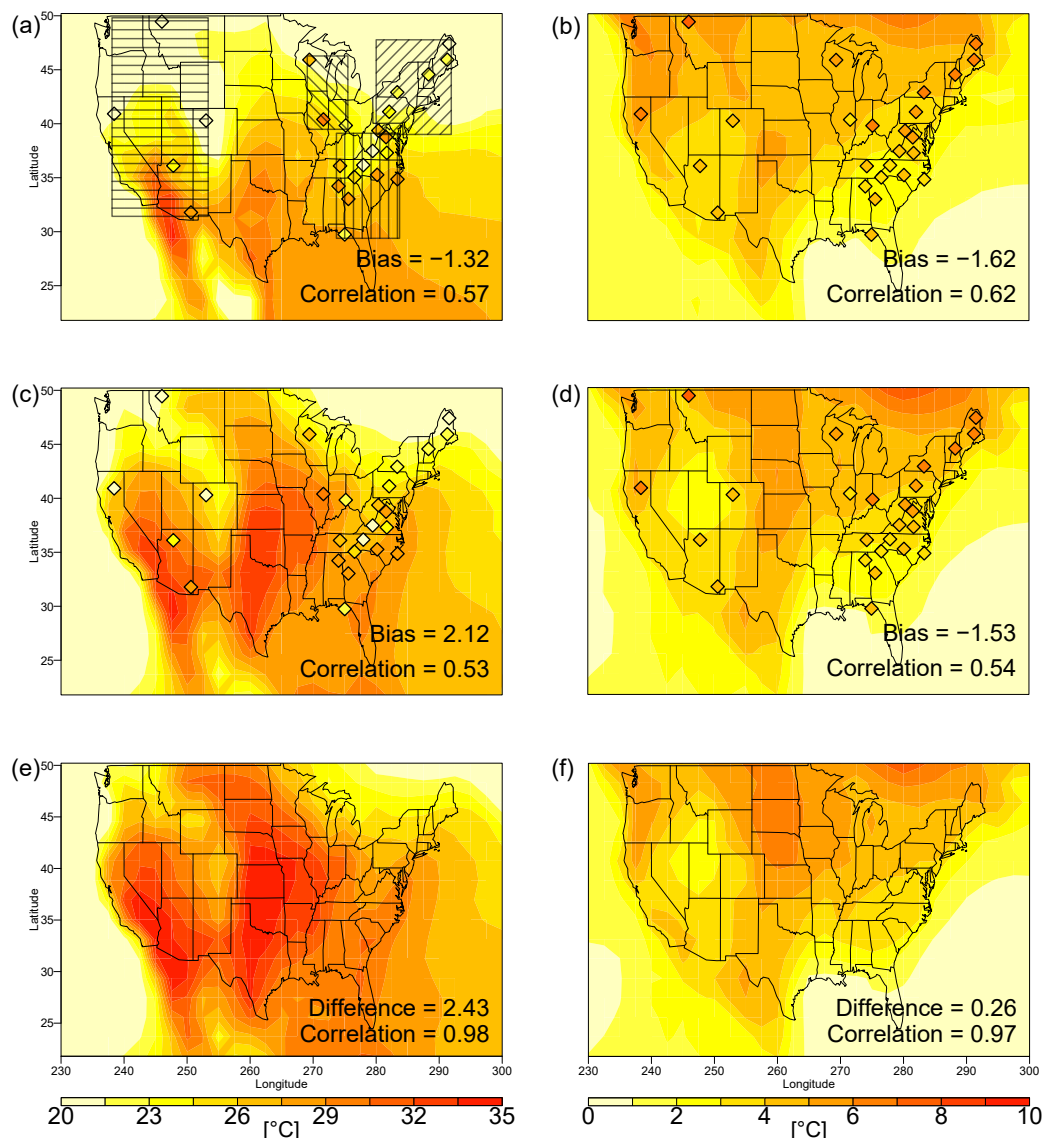
Atmospheric
Chemistry
and Physics
Discussions

Open Access

Figure 2. [Rescaled Data] Average temperature ($^\circ C$) (left column), and average temperature ($^\circ C$) conditioned on temperature greater than the 90th percentile minus average temperature (right column) for the REFC1SD simulation (1992-2010) (first row), the GCM2000 simulation (2006-2025) (second row) and the GCM2100 simulation (2106-2125) (third row). CASTNET measurements (1992-2011) of each quantity are shown as filled diamonds in the first two rows. In the first two rows we also give: the average bias as the model average minus the CASTNET average for each quantity, and the correlation as the spatial correlation between the model and the CASTNET measurements. In the last row we give: the difference as the mean difference between GCM2100 and GCM2000 over the continental area between $21^\circ N$-$51^\circ N$ and $230^\circ E$-$300^\circ E$ and the correlation as the correlation between GCM2100 and GCM2000 over the continental area between $21^\circ N$-$51^\circ N$ and $230^\circ E$-$300^\circ E$. The boxes in (a) show the division of the country into various regions: the Northeast, the Southeast, the midwest and the west.
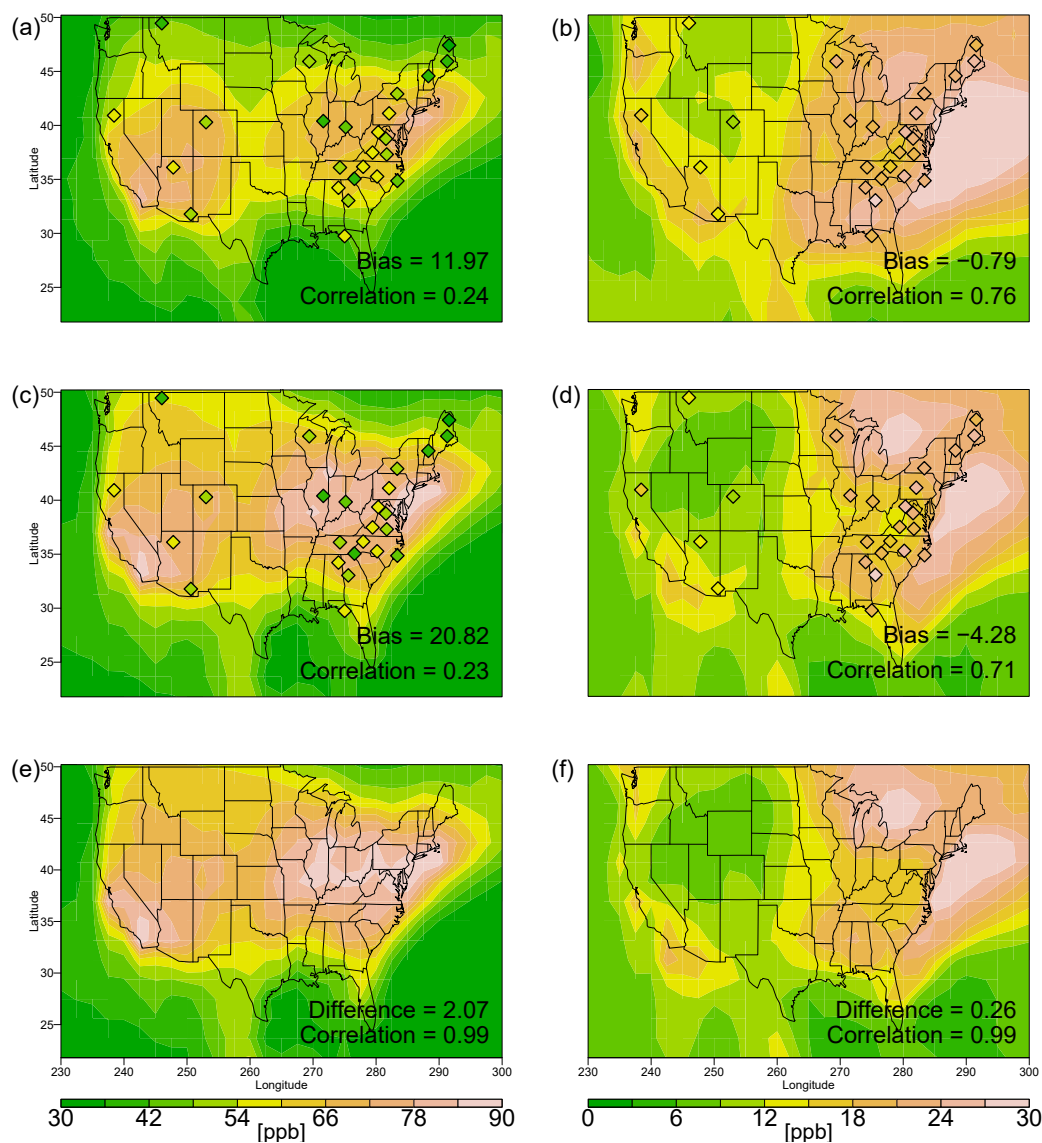
Figure 3. [Rescaled Data] Average ozone (ppb) (left column), and average ozone (ppb) conditioned on ozone greater than the 90th percentile minus average ozone (right column) for the REFC1SD simulation (1992-2010) (first row), the GCM2000 simulation (2006-2025) (second row) and the GCM2100 simulation (2106-2125) (third row). The biases, differences and correlations are defined similarly to Fig. 2.

than 1, extending from the southeast US northwestward to the midwest corresponds quite close to where $\Psi(T,T)$ is greater than 1. The overall correlation between these quantities is 0.3, significant, but weak. There have been varying predictions for whether future ozone increases in the extreme (e.g., Sun et al. (2017)). Figure 4a suggests that in only a few locations in a future climate does the 90th percentile ozone concentration increase by at least 10% over the increase in the median.
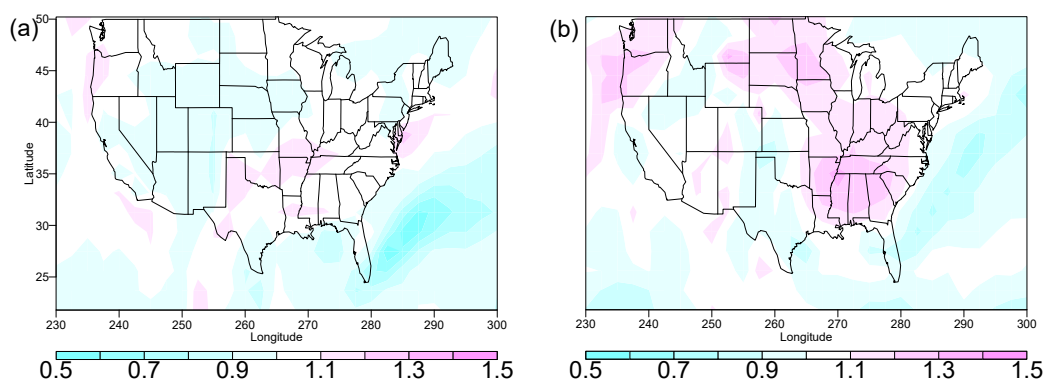

Figure 4. [Rescaled Data] a) $\Psi(O_3, O_3)$, b) $\Psi(T,T)$. (See the definition of Ψ in (7)).

5   Return levels are used to describe the marginal extremes. Return levels are calculated using the procedure given in Phalit-nonkiat et al. (2016) (see Appendix A for more detail). Differences between the 20-year return ozone concentration and the mean concentration are generally higher in the eastern US than in the western US (Fig. 5), consistent with Fig. 3b, d, and f. This difference is dramatically underestimated in the GCM2000 simulation in all regions of the country, and in the northeastern and southeastern regions in the REFC1SD simulation (Table 3). Overall, the difference between the simulated 20-year return

10   period ozone and the mean ozone are biased low by approximately 7 ppb in the REFC1SD simulation and 13.5 ppb in the GCM2000 simulation (Fig. 5 and Table 3). This underestimation suggests that the simulations do not capture the observed high-end range of the ozone extremes. Note that while the simulations underestimate the differences between the 20-year re-turn ozone concentration and the mean concentration, in the northeast and southeast, the actual 20-year return levels for ozone are similar in the measurements and in the REFC1SD and GCM2000 simulations (Table 3). However, this agreement can be

15   attributed in part to the fact that the simulations have a considerable ozone bias in the mean (Fig. 3 and Table 2). In the west and particularly the midwest, both the REFC1SD and GCM2100 simulations substantially overpredict the 20-year return period of ozone (Table 3). Future changes in the 20-year return period ozone and the mean ozone between the GCM2100 and GCM2000 simulations are small. The future difference between the 20-year return concentrations and the mean concentrations decrease slightly when averaged over all measurement sites and increase slightly when averaged over the continental US (Table 3 and

20   Fig. 5). This result is consistent with Rieder et al. (2015), but is at odds with a number of studies that suggest future ozone levels will increase primarily at the high end due to the impact of climate (e.g., Wu et al. (2008)).

Simulated differences between 20-year return temperatures and mean temperature occur primarily in the northern part of the domain and extend southwards through the midwest consistent with Fig. 2, consistent with Fig. 5 and Table 3. The GCM2000

simulation generally captures the measured 20-year return temperature levels but is biased low in the difference between the 20-year return temperature and the mean temperature level (Fig. 5 and Table 3). The REFC1SD simulation is biased low in both quantities. The GCM2100 temperatures (Fig. 2) and 20-year temperature return levels increase (Table 3), with a relatively small increase in the temperature difference between the 20-year return value and the mean temperature. A comparison of the

5   distribution tail for both ozone and temperature is given in Appendix C.

4.2   Joint dependence of temperature and ozone

In this section, we examine the joint dependence of ozone and temperature in the three simulations and in the data. In particular, we are interested in how high ozone events are related to high temperature events in the present and future climates. We use three measures to quantify this dependence and to compare it between the future and present climates: conditional correlation,

10   and using the metrics: Ψ and φ.

- We analyze the correlation between ozone and temperature to measure the overall linear correlation of ozone and temperature between these fields. We also analyze the correlation between ozone and temperature conditioned on temperature greater than the 90th percentile to measure the relationship of ozone and temperature at higher temperatures.

- The quantity $\Psi(O_3, T)$ measures the relative response (against the mean response) of ozone at the 90th percentile level

15   to temperature at the 90th percentile level in the future versus present climate (Eq. (7)).

- The quantity φ gives an explicit relationship between ozone and temperature extremes (Eq. (6)).

The simulated correlation between temperature and ozone is high over sections of the northwestern states, the Rockies and the Southeast in all simulations (Fig. 6a, c, f). The correlations in the REFC1SD simulation and the GCM2000 simulation are rather distinct geographically. Based on the rather sparse CASTNET measurements, it is difficult to determine which simulation

20   better captures the true correlation pattern. The conditional correlations between ozone and temperature when temperature is greater than the 90th percentile are significantly reduced across the country in comparison with the unconditional correlations. Measured conditional correlations are, in all cases, marginally positive or negative. The simulated conditional correlations are somewhat higher, particularly in the eastern part of the country and in the REFC1SD simulation. The simulated conditional correlations maximize in the gulf coast states. Shen et al. (2016) shows a suppression of ozone at high temperatures at many

25   sites across the US.

A metric for the response of ozone to high temperatures can be defined as ozone (ppb) conditioned on temperature greater than the 90th percentile minus average ozone (Fig. 7a, b, c). The largest simulated response to temperature extremes extends off the eastern seaboard to the Southeastern US in all simulations. This is despite the fact that the temperature variability (as measured by $mean(T|T > 90\%) - mean(T)$) is comparatively low in the Southeast US. The overall simulated bias of ozone

30   conditioned on temperature above the 90th percentile is relatively small in both the REFC1SD and GCM2000 simulations. This small bias is somewhat surprising, given the biases enumerated above in simulated ozone, temperature and their variability. The two inland CASTNET sites in the Southeast provide some validation to the simulated pattern as do the relatively
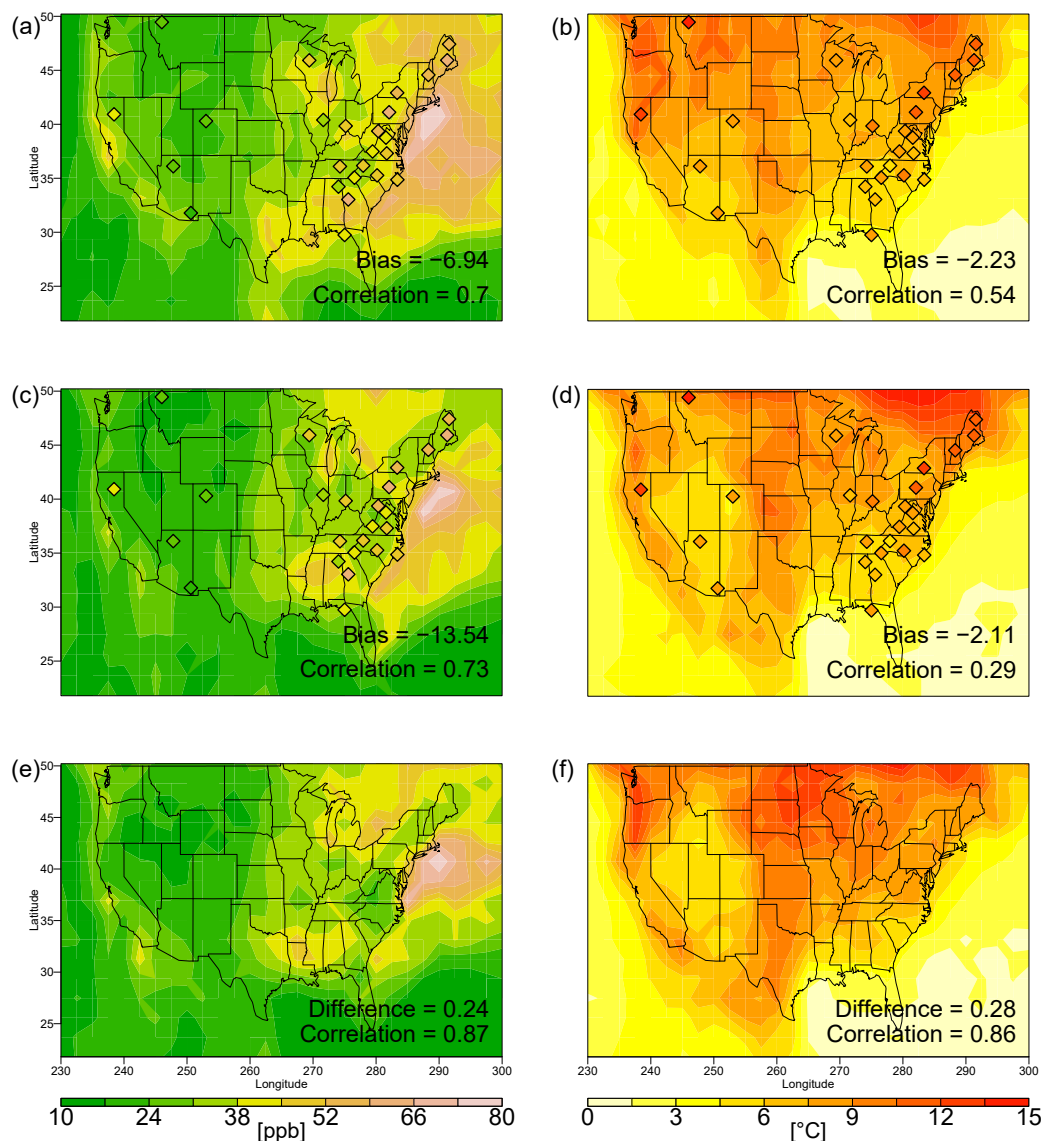
Figure 5. [Rescaled Data] Twenty-year return level minus average ozone (ppb) (left column), 20-year return level minus average temperature (°) (right column) for the REFC1SD simulation (1992-2010) (first row), the GCM2000 simulation (2006-2025) (second row) and the GCM2100 simulation (2106-2125) (third row). Twenty-year return levels from CASTNET measurements (1992-2011) for each quantity are shown as filled diamonds in the first two rows. The bias and correlation in the first two rows and the difference and correlation in the last row are defined as in Fig. 2.
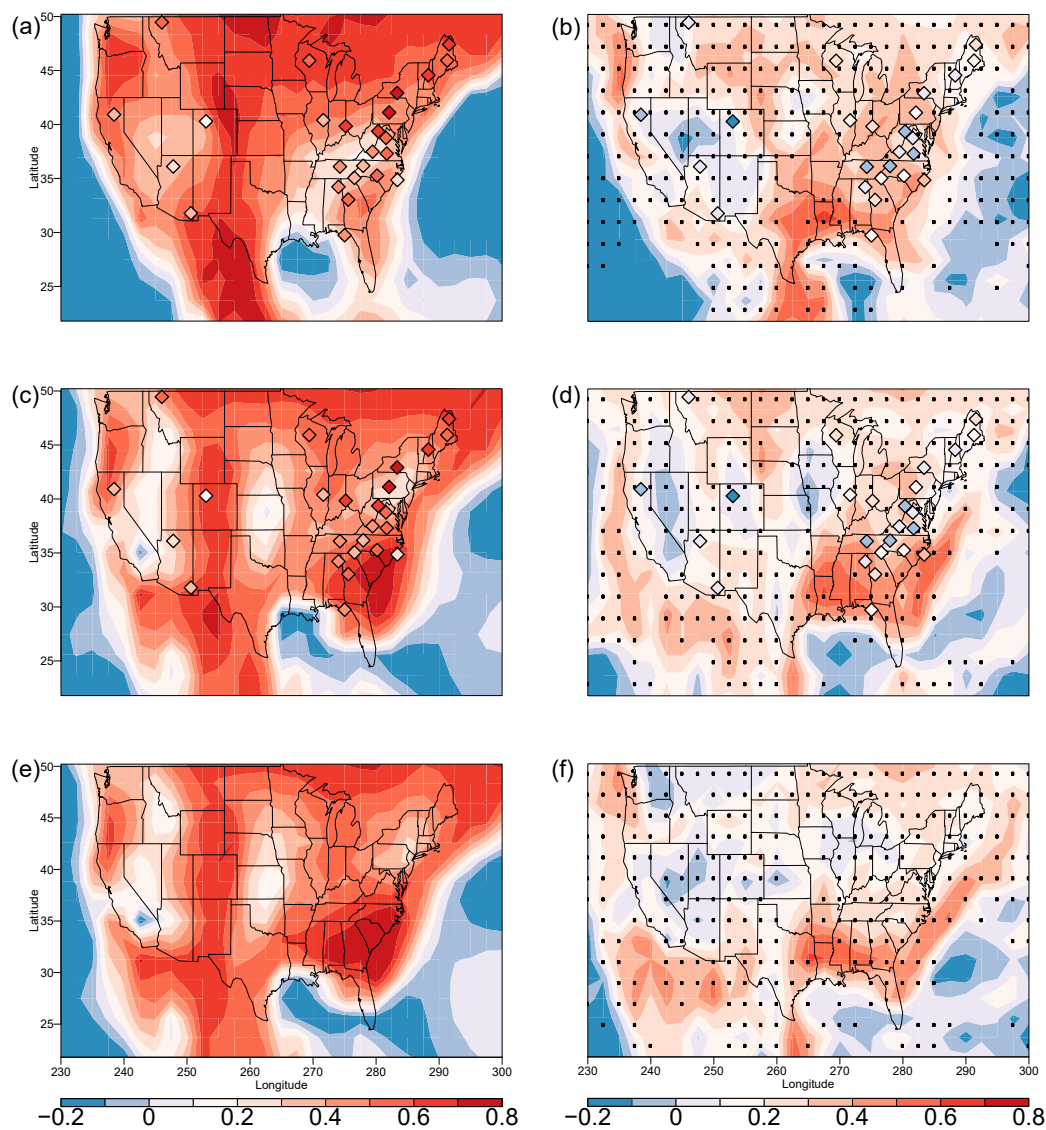
Atmospheric
Chemistry
and Physics

Discussions

Figure 6. [Deseasonalized Data] Unconditional correlations between temperature and ozone (first column); correlations between temperature and ozone conditional on temperature greater than the 90th percentile (second column), for the REFC1SD simulation (1992-2010) (first row), the GCM2000 simulation (2006-2025) (second row) and the GCM2100 simulation (2106-2125) (third row). The unconditional and conditional correlations from CASTNET measurements (1992-2011) are shown as filled diamonds in the first two rows. The black dots on the right panels indicate the significant changes from the unconditional to conditional correlations.

high model-measurement correlations. However, the results do seem somewhat at odds with Shen et al. (2016) who find that temperature in the Southeast does not improve their statistical model of ozone exceedances. Note that the REFC1SD and the GCM2000 simulations show similar responses in the Southeast even though the REFC1SD simulation includes interactive isoprene emissions, while the GCM simulations do not. The measurements also indicate that a high ozone response to tem-

5 perature extremes is found in the Northeastern US extending to Ohio. This measured response is simulated to some extent in the REFC1SD simulation, but not well captured in the GCM2000 simulation (Fig. 7a, b). Overall both the REFC1SD and GCM2000 simulations show a small bias in their response to high temperatures, 0.61 and -1.13 ppb, respectively.
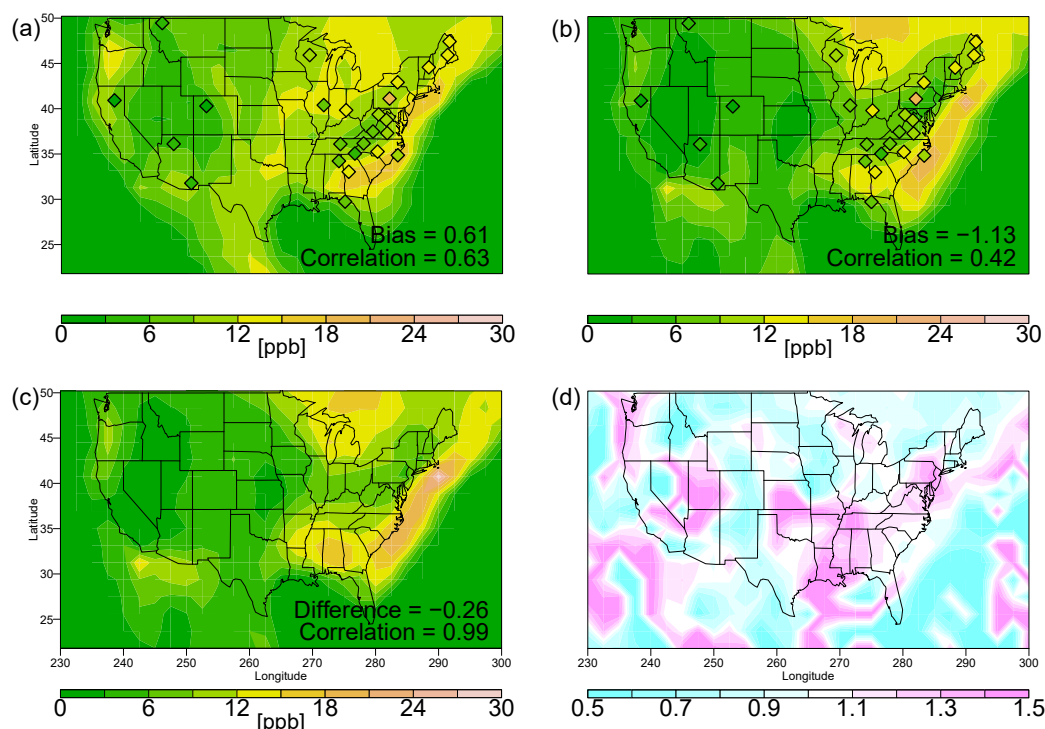

Figure 7. [Rescaled Data] Average ozone (ppb) conditioned on temperature greater than the 90th percentile minus average ozone for (a) the REFC1SD simulation (1992-2010), (b) the GCM2000 simulation (2006-2025) and (c) the GCM2100 simulation (2106-2125). The biases, differences and correlations are defined similarly to Fig. 2. (d) $\Psi(O_3, T)$ (See the definition of Ψ in (7)).

Averaged over the continental US, ozone conditioned on temperature greater than the 90th percentile minus average ozone (Fig. 7c) decreases modestly by 0.26 ppb between GCM2000 and GCM2100. Given the 2.07 ppb future increase in mean

10 ozone (see Fig. 3) this implies ozone conditioned on the 90th percentile of mean temperature increases by 1.81 ppb. This is again consistent with a suppression of ozone at high temperatures at many sites across the US. The comparative sensitivity to temperature increases in GCM2100 versus GCM2000 can be assessed with $\Psi(O_3, T)$ (equation 7). While most of the country suggests future decreases in temperature sensitivity a number of regions, including the gulf coast states and the Pacific

northwest, show an increase in sensitivity by over 30% (Fig. 7d). Both of these regions also show an increase in $\Psi(O_3, T)$ (Fig. 4b).

Measured and simulated scatter plots of deseasonalized ozone versus temperature are shown for three CASTNET sites in
Fig. 8. In each plot, the extreme points after the normalization by the ranks method (see Appendix B for the detailed procedure) are shown in red. As described above (Sect. 3) the extremal dependence between the two variables is characterized by φ, where φ gives the proportion of the extreme points where both variables are simultaneously extreme. At Ashland Maine (Fig. 8a), all model simulations underestimate the extreme dependence of ozone on temperature, where about 25% of the measured points have simultaneous ozone and temperature extremes; at Sand Mountain Alabama (Fig. 8b), all model simulations overestimate
the extreme dependence, where approximately 9% of the measured data have simultaneous ozone and temperature extremes; at Beaufort North Carolina (Fig. 8c), about 20% of the simulated and measured extremes occur simultaneously for temperature and ozone.

The measured sites where ozone and temperature extremes tend to co-occur (Fig. 9) in the Northeastern US and in the Southeastern US are obviously related to those sites where ozone shows the most response to high temperatures (Fig. 7a, b).
Schnell and Prather (2017) find the co-occurence of temperature and ozone extremes also maximize over the Northeast US. They also find a secondary maximum of less amplitude over the Southeastern US consistent with our analysis. However, Schnell and Prather (2017) do not find the spine of low co-occurences clearly seen in the CASTNET data from northern Alabama to Pennsylvania. The GCM2000 simulation does not capture the measured high co-occurences of ozone and temperature in the Northeast US while the REFC1SD simulation does somewhat better (Fig. 9a, b) analogous to the comparison in Fig. 7.
There are also large differences between REFC1SD simulation and the GCM simulations in the midwestern US although the CASTNET measurements are not of sufficient density to evaluate the simulations in the midwest. The student's t-test suggests that the GCM2000 fails to capture the extreme dependence between temperature and ozone at the 95% level; in the REFC1SD simulation we cannot reject with the 95% confidence interval the null hypothesis that the simulated and measured φ are the same. Consistent with measurements, all simulations including GCM2100 show the maximum co-occurence of temperature
and ozone maximum in the Southeastern US. It is in this region that the co-occurence of ozone and temperature maxima increase in the future (Fig. 9d).

5 Discussion

Three simulations using CAM4-chem were analyzed: the Chemistry Climate Model Initiative (CCMI) reference experiment using specified dynamics (REFC1SD) between 1992-2010, a 25-year present-day simulation branched off the CCMI REFC2
simulation in the year 2000 and a 25-year future simulation branched off the CCMI REFC2 simulation in 2100. The average global mean temperature change between the present-day simulation (GCM2000) and the future simulation (GCM2100) simulation is $2.1°C$, less than the $2.8°C$ difference in the parent CCMI REFC2 simulations. The difference in these simulations is most likely attributable to the fact the GCM2100 simulation includes the effect of increased CO2 forcing in the future, but does not account for the impact of projected future aerosol decreases. Thus, in the GCM2100 simulation the relatively large aerosol
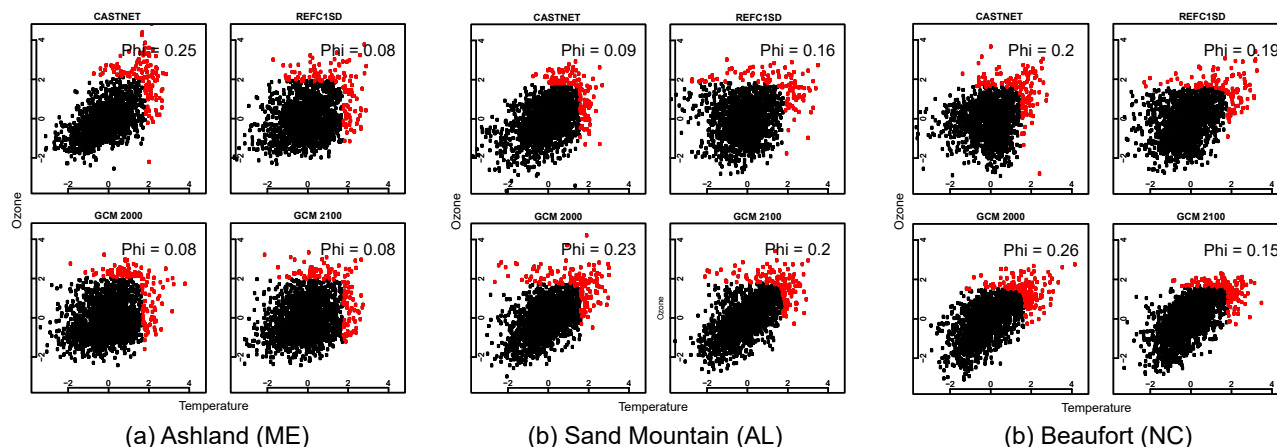
Atmospheric
Chemistry
and Physics
Discussions

Open Access

Figure 8. [Deseasonalized Data] The scatter plots of temperature and ozone from selected CASTNET sites (or the corresponding grid point for the models). (a) Ashland (ME), (b) Sand Mountain (AL), (c) Beaufort (NC). Extreme points picked if the transformed points by using the ranks method are outside the unit circle (see the ranks method in Appendix B).

radiative forcing acts as a buffer against the increased CO2. Over the continental US ozone increases by approximately 2.1 ppb between the GCM2000 simulation and the GCM2100 simulation. Future ozone increases in GCM2000 as the projected future decrease in ozone precursors is not accounted for. This is probably countered, to some extent, by the relatively low future temperatures.

Both the REFC1SD and GCM2000 simulations underestimate the width of the present-day ozone and temperature distributions and thus do not adequately capture the measured extremes with respect to their means. Overall, the difference between the 20-year return level temperature and the mean temperature is underestimated by nearly $2.2°C$ in the REFC1SD simulation and $2.1°C$ in the GCM2000 simulation; for ozone the difference between the 20-year return level ozone and mean ozone is underestimated by 6.9 ppb and 13.5 ppb in the REFC1SD and GCM2000 simulations, respectively. Finer resolution may reduce the ozone bias, but it is unclear whether it better captures the extremes (see Pfister et al. (2014)).

Interestingly, despite the large bias in mean ozone in the REFC1SD and GCM2000 simulations in the NE US (14 ppb and 21 ppb, respectively) and in the SE US (10 ppb and 20 ppb, respectively) the simulated 20-year ozone return levels in these regions show little bias.

The simulations show a fundamental mismatch between the locations where the width of the right hand side (rhs) of the temperature distribution is large and those locations where the width of the rhs of the ozone distribution is large. As measured by the difference between the 20-year return temperature and the mean temperature (Fig. 5) (or the difference between the 90th percentile temperature and the mean temperature, Fig. 2) the width of the rhs of the temperature distribution is highest in the northern portion of the domain with a southward extension through the midwestern states. This pattern is consistent with increased temperature variability at higher latitudes (e.g., Deser et al. (2012) and references therein) and a higher temperature
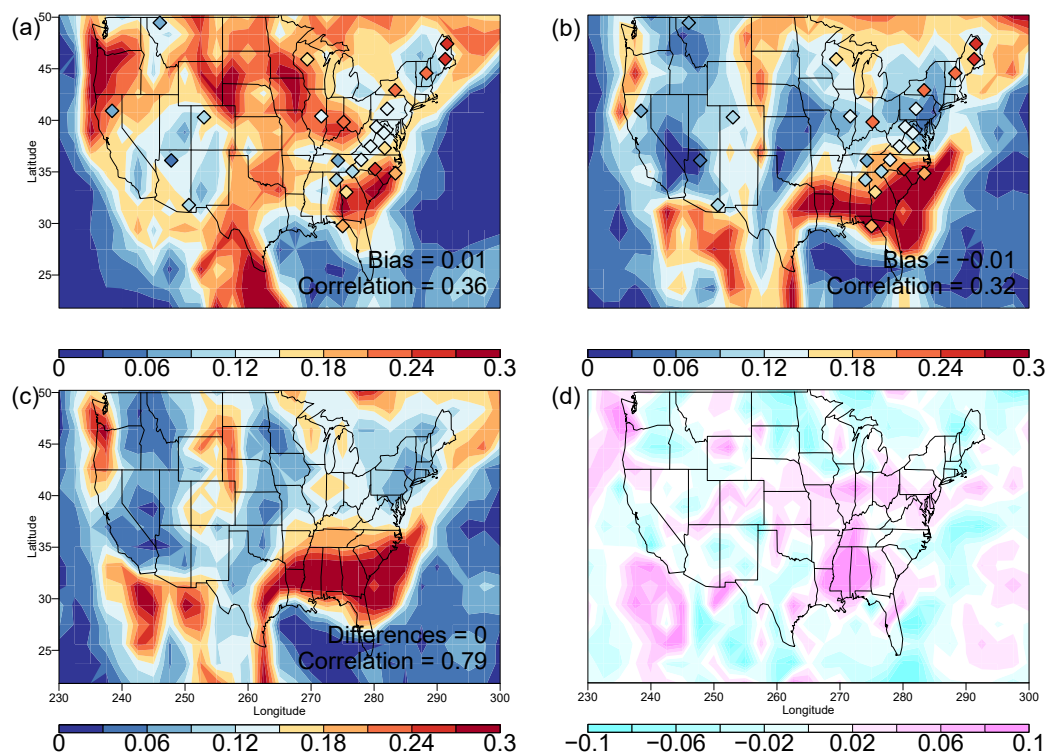
Figure 9. [Deseasonalized Data] Areas φ from (a) REFC1SD simulation (1992-2010), (b) GCM2000 simulation (2006-2025), (c) GCM2100 simulation (2106-2125). Areas φ from CASTNET measurements (1992-2011) are shown as filled diamonds in (a) and (b). The bias and correlation in (a), (b) and the difference and correlation in (c) are defined as in Fig. 2. (d): Area φ from GCM2100 simulation (2106-2125) minus areas φ from GCM2000 simulation (2006-2025).

variance in interior of the country due its greater continentality. On the other hand, the 20-year return levels for ozone minus the ozone mean (Fig. 5) (or the 90th percentile ozone minus the ozone mean, Fig. 3) indicate the width of the rhs of the ozone distribution is highest in the eastern third of the country. Thus in many locations, the width of the rhs of the ozone distribution

5   is not determined by the width of the rhs of the temperature distribution. The overlap or lack of overlap between the regions of high temperature and high ozone variability impacts the relationship between these two quantities.

The ozone and temperature fields are not well correlated in the GCM2000 simulation in the region of maximum temperature variability in the central part of the country (Fig. 6). φ (measuring the joint extremes of ozone and temperature) is also relatively small there (Fig. 9). In these regions changes in temperature are not likely to give a large response in ozone with important

10   implications for the response of ozone to heat waves. However, the REFC1SD simulation gives a notably different response. In the REFC1SD simulation, the correlation between temperature and ozone (Fig. 6) and the joint extreme distribution of ozone and temperature (φ) is much larger in the central Midwest than in the GCM2000 simulation. Measurements at the CASTNET sites are not sufficiently dense in this region of the country to resolve the discrepancy between the GCM2000 and the REFC1SD

simulations. However, correlations between ozone and maximum temperature using the EPA Air Quality System (EPA-AQS) show small ozone-temperature correlations along the gulf coast but higher correlations in the interior Midwest, more in line with the REFC1SD simulation (Shen et al. (2016)).

5   These differences between the REFC1SD and GCM2000 simulations are likely due to meteorological differences: while The REFC1SD simulation is driven with analyzed meteorology, the GCM2000 simulation is driven with model calculated meteorology. In particular, we hypothesize that these differences may be due to a poor simulation of the Bermuda high in the CGM2000 simulation. The position of the Bermuda High strongly impacts ozone distribution over the U.S. (Zhu and Liang (2013)) with the second empirical orthogonal function of ozone variability strongly correlated with the location of the Bermuda

10   High (Shen et al. (2016)). A westward extension of the Bermuda high is correlated with high temperatures and low ozone over the much of the Southeast US (Zhu and Liang (2013)) consistent with the correlation between ozone and temperature in the REFC1SD simulation (Fig. 6). In the GCM2000, the Bermuda High is simulated too far to the west (not shown). A maximum covariance analysis shows that the mode of variability associated with the Bermuda High is also displaced too far to the west (not shown). Thus, the pattern of variability associated with the Bermuda high is incorrectly simulated in the GCM2000

15   simulation. Zhu and Liang (2013) show the Bermuda high is not well simulated in the majority of GCMs. This has important implications for the simulation of the ozone response to temperature and thus to heat waves in large regions of the country.

In this study, we introduce a new spectral method using multivariate extreme value theory to measure extremal dependence between temperature and ozone in both the observations and model simulations. We find through the use of this new metric joint extremes of temperature and ozone occur together up to approximately 35% of the time in a few regions, although on

20   average their joint occurrence is significantly less. Previous studies have used different methodologies to capture the extremal dependence between ozone and temperature. Sun et al. (2017), calculated the conditional probability of a high ozone day (ozone above the 90th percentile) given a high temperature day (temperature above the 90th percentile). They found probabilities that ranged from approximately 50% in the northeastern U.S. to somewhat less than 20% in the western U.S. Schnell and Prather (2017) and Zhang et al. (2017), calculated the joint probability that ozone and temperature are high (above the 95th percentile)

25   compared to the probability that either one of them is high. Our measurement analysis is in qualitative agreement with Schnell and Prather (2017) but due to the different methodologies the quantitative results are not strictly comparable. Schnell and Prather (2017) also find that the co-occurrence of temperature and ozone extremes maximize over the Northeast US (occurring 50% or more of the time in their analysis) but decrease towards the Midwest (where joint occurrences occur 25% or less of the time). They also find a secondary maximum of less amplitude in the joint occurrence of extremes over the Southeastern

30   US consistent with our analysis. However, Schnell and Prather (2017) do not find the spine of low co-occurrences clearly seen in the CASTNET data from northern Alabama to Pennsylvania in our analysis. Zhang et al. (2017) find the co-occurrence of extreme ozone and temperature occurs 32% of the time averaged over the U.S. with a maximum over the Northeastern U.S. The advantage of the method discussed here for finding joint extremes of temperature and ozone is that it gives detailed information about the joint extremes and is not restricted to a particular quantile of the distribution. It can be used to forecast joint extremes even out of the range of available samples.

Atmospheric
Chemistry
and Physics
Discussions

The CASTNET measurements show the southeast and northeast regions have the largest response of ozone to temperature extremes $(mean(O_3|T > 90\%) - mean(O_3))$ (Fig. 7). The CASTNET measurement sites in the far southeastern part of the country have small measured variations in relative extreme temperature $(mean(T|T > 90\%) - mean(T))$ but large

5 variations in relative extreme ozone $(mean(O_3|O_3 > 90\%) - mean(O_3))$. Thus, in the southeastern US the sensitivity of ozone to changes in temperature are relatively large. Over the northeastern US both the relative variations in extreme ozone $(mean(O_3|O_3 > 90\%) - mean(O_3))$ and temperature $(mean(T|T > 90\%) - mean(T))$ are relatively high. In this region, the ozone sensitivity to temperature change is relatively small.

The northeast and southeast regions, the regions with the large ozone response to temperature extremes, have the highest

10 spectral dependence between ozone and temperature extremes (Fig. 9) and the highest correlations between temperature and ozone, conditioned on temperature greater than the 90th percentile level (Fig. 6). In general, the REFC1SD simulation captures the measured relations between ozone and temperature better than the GCM2000 simulation over the northeast US, although it does not fully capture their strong measured relationship (e.g., see Fig. 6). In the southeast the measured response appears to be generally well simulated in both simulations. Overall the GCM2000 fails to capture the extreme dependence as measured

15 by φ between temperature and ozone at the 95% level; in the REFC1SD simulation we cannot reject the null hypothesis that the simulated and measured values are the same.

Due to the strong dependence of ozone on temperature, future ozone and its extremes may depend on changes in temperature and its extremes. While the future temperature increases everywhere in relation to the current climate, in many places the width of the rhs of the future temperature distribution decreases. The future difference between summertime extreme temperatures

20 (at the 90th percentile) and mean temperatures increases by up to 20 to 30% compared to present day differences $(\Psi(T,T))$ over parts of the southern Mississippi basin extending to the northern Midwest and the Northwest coast (Fig. 4). The pattern of this increase bears a striking resemblance to those locations where measured summertime interannual extreme temperatures increase relative to interannual increases in the mean (Huybers et al. (2014)), a process linked to drying of the soils (Huybers et al. (2014)). In other parts of the country the relative future increase is small or negative. Note that the increase in $(\Psi(T,T))$

25 over the lower Mississippi valley occurs in a location strongly impacted by the Bermuda High and thus warrants further investigation. Note also, this increase occurs in those locations where the REFC1SD simulation gives a low correlation between ozone and temperature.

To what extent are the relative changes in the future width of the ozone distribution determined by the relative future changes in that of the temperature distribution? The correlation between $\Psi(T,T)$ and $\Psi(O_3,O_3)$ is significant, but weak, with

30 a correlation coefficient of 0.3. This suggests a weak relationship between changes in the right-hand side of the future ozone distribution and the future temperature distribution. Overall, future ozone is less responsive to temperature than present day ozone $(mean(O_3|T > 90\%) - mean(O_3))$ but the effect is small averaged over the continental US (-0.26 ppb) suggesting only relatively modest temperature suppression. The ratio of future sensitivities to temperature compared to present varies regionally ranging from -50% to +50% (Fig. 7). Interestingly, ozone does become more responsive to temperature changes in the lower

35 Mississippi valley (Fig. 7), in precisely the region that the width of the temperature distribution increases (Fig. 4). However,

even in this region the rhs of the future ozone distribution does not become significantly wider than its present day values (Fig. 4).

There have been different predictions as to whether climate change increases future ozone extremes with respect to the increase in the mean (e.g., see Sun et al. (2017)). On average the width of the rhs of the future ozone distribution increases

5   slightly by 0.26 ppb in the future simulation ($mean(O_3|O_3 > 90\%) - mean(O_3)$) (Fig. 2, but also see Fig. 5 for the relative change in the 20-year return level), but in many locations the relative width decreases ($\Psi(O_3, O_3)$, Fig. 4). Where it increases, the increase is always less than 20%. Our results generally suggest that the increase in future ozone is primarily due to a shift in the ozone distribution and not due to an increase in ozone at the high end.

6   Conclusion

10   We investigate high temperature and ozone extremes and their joint occurrence over the United States during the summer months (JJA) in measurements and simulations of the present and future climate. Two present-day simulations are analyzed using CESM1 CAM4-chem: (i) the CCMI REFC1SD simulation (1992-2010) driven by MERRA meteorology and (ii) a 25-year online simulation (GCM2000) branched off from the present-day CCMI REFC2 simulation (where CO2 is set at 369 ppm). In addition, a future simulation using CAM4-chem is branched off from the future CCMI REFC2 simulation (GCM2100)

15   with a specified CO2 concentration of 669 ppm following the RCP6 scenario. Distinct from the CCMI REFC2 simulations the emissions and long-lived greenhouse gas distributions (except CO2) are held constant in the GCM2000 and GCM2100 simulations at values representative of the year 2000. Statistics of the maximum 8 hour averaged ozone and maximum daily temperature distributions are compared in the REFC1SD and GCM2000 simulations against measurements at CASTNET sites. To render the data approximately stationary on both the inter-annual and seasonal basis, the temperature and ozone data are

20   scaled.

Scaled temperature biases as evaluated at the CASTNET sites are $-1.3°C$ and $2.1°C$ in the REFC1SD and GCM2000 simulations, respectively. Scaled ozone biases are 12 and 21 ppb respectively. Consistent with many global model simulations the ozone bias is particularly pronounced over the Eastern U.S. In all regions of the US both the REFC1SD and the GCM2000 simulations underestimate the 20-year return period of ozone (temperature) minus mean ozone (temperature): the underestimate

25   for ozone in the GCM2000 simulation is over 9 ppb in all regions of the country and exceeds 20 ppb in the northeast; the underestimate for temperature is generally about $2°C$.

The main conclusions from this study are as follows:

–   Both the REFC1SD and GCM2000 simulations underestimate the measured tail on the high end of the temperature and ozone distributions. The GCM2000 simulation simulates the temperature extremes better than the REFC1SD simulation,

30   but the REFC1SD simulation significantly underestimates the tail of the ozone distribution. Further comparison of simulation differences between CAM4-chem with specified dynamics and CAM4-chem run with online meteorology are given in Brown-Steiner et al. (2015).

Atmospheric
Chemistry
and Physics
Discussions

Open Access

EGU

– We propose a new method to measure the joint extremes of temperature and ozone by calculating the spectral density (φ) of the joint extremes of ozone and temperature. This measure of the joint extremes is not restricted to a particular quantile of the distribution, but can be used to forecast joint extremes even out of the range of available samples. Observations show that φ is highest in the northeast US and in the southeast US consistent with the ozone response to extreme temperatures ($mean(O_3|T > 90\%) - mean(O_3)$), and the correlation between ozone and temperature conditioned on temperature greater than the 90th percentile.

– There is a geographical mismatch between where the simulated high temperature extremes occur and the high ozone extremes (as measured by the 20-year return values minus the mean). Thus, while ozone concentrations are often correlated with temperature, the regions of high ozone extremes do not necessarily match the regions of high temperature extremes. In the southeast the relative temperature extremes ($mean(T|T > 90\%) - mean(T)$) are small but the relative ozone extremes are large.

– The REFC1SD and the GCM2000 simulations show discrepancies in the measured relation between ozone and temperature. The response of the REFC1SD simulation is qualitatively better than that of the GCM2000 simulation. We hypothesize that the differences in these simulations are meteorologically induced and may, at least in part be attributed to a poor simulation of the Bermuda High in the GCM2000 simulation. These differences suggest that ozone will respond rather differently to heat waves in the two simulations.

– In the future climate the ozone and temperatures distributions shift to the right. However, in many locations the right hand side of both distributions become narrower (e.g., for ozone $mean(O_3|O_3 > 90\%) - mean(O_3)$ decreases in the future). Our results generally suggest that the increase in future ozone is primarily due to a shift in the ozone distribution and not due to an increase in ozone in the extremes. The correlation between relative changes in the high end of the future temperature distribution ($\Psi(T,T)$) and the ozone distribution ($\Psi(O_3,O_3)$) is 0.3.

Appendix A: Univariate regular variation

To understand the basic characteristics of extreme distributions, we should introduce the notion of *regular variation*. A regularly varying function is a function whose behavior at infinity follows a power law function. That is, a regularly varying function with an index α can be explained by

$$\lim_{t \to \infty} \frac{F(tx)}{F(t)} = x^{\alpha}, \tag{A1}$$

for all $x > 0$.

Regularly varying functions are studied in many fields and one of the applications that we will use here is to estimate the tail indices α of extreme ozone and extreme temperature distributions in order to estimate N-year return levels of those variables. Alternatively, we can fit the ozone or temperature distributions to the Generalized Pareto Distribution (GPD) and estimate the

Atmospheric
Chemistry
and Physics
Discussions

Open Access

shape parameters which are equivalent to the reciprocal of the tail indices (shape $= \alpha^{-1}$) if the shape parameter is positive. Phalitnonkiat et al. (2016) suggests a procedure to estimate shape parameters using a combination of Hill estimators and MLEs.

Appendix B: Ranks method

Let us consider 2-dimensional random vectors (X, Y). When the tail part of X's distribution and the tail part of Y's distribution are independent, we would expect that X and Y are unlikely to yield extreme values at the same time, and vice versa. This observation suggests that when we plot only extreme points from (X, Y), the points would appear to be around the axes if X and Y are extreme independent, and vice versa. This is actually true in higher dimensions as well. However, the tool described above for measuring the dependence between variables only applies to variables with the same marginal tail indices.

Among the methods suggested by Resnick (2007), we use a transformation that essentially normalizes the tail indices of all components to 1 without calculating or estimating the tail indices α_j for each $j = 1, ..., d$. This method is called the *Ranks methods*. The major benefit from this method is that we can avoid the marginal tail index estimation which reduces numerical errors; however, the drawback is that the transformation itself destroys the iid property of the data and makes it more complicated to obtain asymptotic distributions, see Einmahl et al. (2001). The method can be done as follows.

Let $\mathbf{X}_i = (X_i^{(1)}, ..., X_i^{(d)}), i = 1, ..., n$ be $d-$dimensional vectors. Denote the *rank* of $X_i^{(j)}$ by

$$r_i^{(j)} := \sum_{m=1}^{n} 1_{[X_m^{(j)} \geq X_i^{(j)}]}. \tag{B1}$$

For a fixed $k > 0$ and for each $i = 1, ..., n$ we transform $\mathbf{X}_i$ into a rank vector by

$$\left(X_i^{(1)}, ..., X_i^{(d)} \right) \mapsto \left(\frac{k}{r_i^{(1)}}, ..., \frac{k}{r_i^{(d)}} \right). \tag{B2}$$

We consider a point $\left(X_i^{(1)}, ..., X_i^{(d)} \right)$ as jointly extreme if $\left|\left| \left(\frac{k}{r_i^{(1)}}, ..., \frac{k}{r_i^{(d)}} \right) \right|\right| > 1$, where $||\cdot||$ is a norm in $\mathbb{R}^d$. In this case, we use the L^2-norm. We use the transformed vectors to estimate the spectral measure (or angular measure in the case of 2-dimensional vectors).

Appendix C: Estimating spectral measure

To estimate the spectral measure from the data in 2-dimensional polar coordinates, we measure the angles between the transformed points $\left(\frac{k}{r_i^{(1)}}, \frac{k}{r_i^{(2)}} \right)$ and the x-axis. That is, we can estimate the empirical measure $\hat{S}$ by

$$\hat{S}(A) = \frac{\text{\# of extreme points with angles in } A}{\text{\# of extreme points}}. \tag{C1}$$

Note that this can be extended to higher dimensions in a similar way.

We may notice that the choice of k has a major role on how we categorize extreme points. The higher k is, the more points would lie outside the unit circle, and hence, the more extreme points. We use the procedure from Nguyen and Samorodnitsky (2013) to estimate k.

Atmospheric
Chemistry
and Physics
Discussions

Since the angular measure is normalized (i.e., the area under curve from 0 to $\frac{\pi}{2}$ is 1), we can only consider the area of the 'middle' part, which we define to be between $\frac{\pi}{8}$ and $\frac{3\pi}{8}$. Denote this amount by φ:

$$\varphi := \hat{S}(\left[\frac{\pi}{8}, \frac{3\pi}{8}\right]) \approx \text{area} \left[\frac{\pi}{8}, \frac{3\pi}{8}\right], \tag{C2}$$

5   where the area is defined in a notion of kernel density estimation from the angular measure.

Atmospheric
Chemistry
and Physics
Discussions

References

Brown-Steiner, B., Hess, P., and Lin, M.: On the capabilities and limitations of GCCM simulations of summertime regional air quality: A
diagnostic analysis of ozone and temperature simulations in the US using CESM CAM-Chem, Atmospheric Environment, 101, 134 – 148,
https://doi.org/http://dx.doi.org/10.1016/j.atmosenv.2014.11.001, http://www.sciencedirect.com/science/article/pii/S1352231014008590,
2015.

Collins, M., Knutti, R., Arblaster, J., Dufresne, J.-L., Fichefet, T., Friedlingstein, P., Gao, X., Gutowski, W., Johns, T., Krinner, G.,
Shongwe, M., Tebaldi, C., Weaver, A., and Wehner, M.: Long-term Climate Change: Projections, Commitments and Irreversibil-
ity, book section 12, pp. 1029 – 1136, Cambridge University Press, Cambridge, United Kingdom and New York, NY, USA,
https://doi.org/10.1017/CBO9781107415324.024, www.climatechange2013.org, 2013.

Dear, K., Ranmuthugala, G., Kjellström, T., Skinner, C., and Hanigan, I.: Effects of Temperature and Ozone on Daily Mor-
tality During the August 2003 Heat Wave in France, Archives of Environmental & Occupational Health, 60, 205–212,
https://doi.org/10.3200/AEOH.60.4.205-212, 2005.

Deser, C., Knutti, R., Solomon, S., and Phillips, A. S.: Communication of the role of natural variability in future North American climate,
Nature Clim. Change, 2, 775 – 779, https://doi.org/http://dx.doi.org/10.1038/nclimate1562, 2012.

Einmahl, J. H., Piterbarg, V. I., and de Haan, L.: Nonparametric estimation of the spectral measure of an extreme value distribution, The
Annals of Statistics, 29, 1401–1423, 2001.

Eyring, V., Arblaster, J. M., Cionni, I., Sedláček, J., Perlwitz, J., Young, P. J., Bekki, S., Bergmann, D., Cameron-Smith, P., Collins, W. J.,
Faluvegi, G., Gottschaldt, K.-D., Horowitz, L. W., Kinnison, D. E., Lamarque, J.-F., Marsh, D. R., Saint-Martin, D., Shindell, D. T., Sudo,
K., Szopa, S., and Watanabe, S.: Long-term ozone changes and associated climate impacts in CMIP5 simulations, Journal of Geophysical
Research: Atmospheres, 118, 5029–5060, https://doi.org/10.1002/jgrd.50316, http:https://dx.doi.org/10.1002/jgrd.50316, 2013.

Fiore, A. M., Naik, V., and Leibensperger, E. M.: Air Quality and Climate Connections, Journal of the Air & Waste Management
Association, 65, 645–685, https://doi.org/10.1080/10962247.2015.1040526, http://dx.doi.org/10.1080/10962247.2015.1040526, pMID:
25976481, 2015.

Granier, C., Bessagnet, B., Bond, T., D'Angiola, A., Denier Van Der Gon, H., Frost, G. J., Heil, A., Kaiser, J. W., Kinne, S., Klimont,
Z., Kloster, S., Lamarque, J.-F., Liousse, C., Masui, T., Meleux, F., Mieville, A., Ohara, T., Raut, J.-C., Riahi, K., Schultz, M. G.,
Smith, S. J., Thompson, A., Van Aardenne, J., Van Der Werf, G. R., and Van Vuuren, D. P.: Evolution of anthropogenic and biomass
burning emissions of air pollutants at global and regional scales during the 1980-2010 period, Climatic Change, 109, 163–190,
https://doi.org/10.1007/s10584-011-0154-1, https://hal.archives-ouvertes.fr/hal-00637460, 2011.

Guenther, A., Jiang, X., Heald, C., Sakulyanontvittaya, T., Duhl, T., Emmons, L., and Wang, X.: The Model of Emissions of Gases and
Aerosols from Nature version 2.1 (MEGAN2.1): an extended and updated framework for modeling biogenic emissions, Geosci. Model
Dev., 5, 1471–1492, https://doi.org/10.5194/gmd-5-1471-2012, 2012.

Huybers, P., McKinnon, K. A., Rhines, A., and Tingley, M.: U.S. Daily Temperatures: The Meaning of Extremes in the Context of Non-
normality, Journal of Climate, 27, 7368–7384, https://doi.org/10.1175/JCLI-D-14-00216.1, https://doi.org/10.1175/JCLI-D-14-00216.1,
2014.

Lamarque, J.-F., Emmons, L. K., Hess, P. G., Kinnison, D. E., Tilmes, S., Vitt, F., Heald, C. L., Holland, E. A., Lauritzen, P. H., Neu,
J., Orlando, J. J., Rasch, P. J., and Tyndall, G. K.: CAM-chem: description and evaluation of interactive atmospheric chemistry in the

Community Earth System Model, Geoscientific Model Development, 5, 369–411, https://doi.org/10.5194/gmd-5-369-2012, http://www.geosci-model-dev.net/5/369/2012/, 2012.

5   McKinnon, K. A., Rhines, A., Tingley, M. P., and Huybers, P.: The changing shape of Northern Hemisphere summer temperature distributions, Journal of Geophysical Research: Atmospheres, 121, 8849–8868, https://doi.org/10.1002/2016JD025292, http://dx.doi.org/10.1002/2016JD025292, 2016JD025292, 2016.

Nguyen, T. and Samorodnitsky, G.: Multivariate tail estimation with application to analysis of CoVar, ASTIN Bulletin, 43, 245–270, 2013.

OECD: OECD Environmental Outlook to 2050, https://doi.org/http://dx.doi.org/10.1787/9789264122246-en, /content/book/9789264122246-en, 2012.

Pfister, G. G., Walters, S., Lamarque, J.-F., Fast, J., Barth, M. C., Wong, J., Done, J., Holland, G., and Bruyère, C. L.: Projections of future summertime ozone over the U.S., Journal of Geophysical Research: Atmospheres, 119, 5559–5582, https://doi.org/10.1002/2013JD020932, http://dx.doi.org/10.1002/2013JD020932, 2013JD020932, 2014.

Phalitnonkiat, P., Sun, W., Grigoriu, M. D., Hess, P., and Samorodnitsky, G.: Extreme ozone events: Tail behavior of the surface ozone
15   distribution over the U.S., Atmospheric Environment, 128, 134 – 146, https://doi.org/http://dx.doi.org/10.1016/j.atmosenv.2015.12.047, http://www.sciencedirect.com/science/article/pii/S1352231015306257, 2016.

Porter, W. C., Heald, C. L., Cooley, D., and Russell, B.: Investigating the observed sensitivities of air-quality extremes to meteorological drivers via quantile regression, Atmospheric Chemistry and Physics, 15, 10 349–10 366, https://doi.org/10.5194/acp-15-10349-2015, http://www.atmos-chem-phys.net/15/10349/2015/, 2015.

20   Pusede, S. E., Steiner, A. L., and Cohen, R. C.: Temperature and Recent Trends in the Chemistry of Continental Surface Ozone, Chemical Reviews, 115, 3898–3918, https://doi.org/10.1021/cr5006815, http://dx.doi.org/10.1021/cr5006815, pMID: 25950502, 2015.

Ren, C., Williams, G., Morawska, L., Mengersen, K., and Tong, S.: Ozone modifies associations between temperature and cardiovascular mortality: analysis of the NMMAPS data, Occupational and Environmental Medicine, 65, 255–260, http://www.jstor.org/stable/41220742, 2008.

25   Resnick, S.: Heavy-Tail Phenomena: Probabilistic and Statistical Modeling, Springer, New York, 2007.

Rhines, A. and Huybers, P.: Frequent summer temperature extremes reflect changes in the mean, not the variance, Proceedings of the National Academy of Sciences, 110, E546, https://doi.org/10.1073/pnas.1218748110, http://www.pnas.org/content/110/7/E546.short, 2013.

Rieder, H., Fiore, A., Horowitz, L., and Naik, V.: Projecting policy-relevant metrics for high summertime ozone pollution events over the eastern United States due to climate and emission changes during the 21st century, Journal of Geophysical Research: Atmospheres, 120,
30   784–800, https://doi.org/10.1002/2014JD022303, http://dx.doi.org/10.1002/2014JD022303, 2014JD022303, 2015.

Rienecker, M. M., Suarez, M. J., Gelaro, R., Todling, R., Bacmeister, J., Liu, E., Bosilovich, M. G., Schubert, S. D., Takacs, L., Kim, G.-K., Bloom, S., Chen, J., Collins, D., Conaty, A., da Silva, A., Gu, W., Joiner, J., Koster, R. D., Lucchesi, R., Molod, A., Owens, T., Pawson, S., Pegion, P., Redder, C. R., Reichle, R., Robertson, F. R., Ruddick, A. G., Sienkiewicz, M., and Woollen, J.: MERRA: NASA's Modern-Era Retrospective Analysis for Research and Applications, Journal of Climate, 24, 3624–3648, https://doi.org/10.1175/JCLI-D-11-00015.1,
35   http://dx.doi.org/10.1175/JCLI-D-11-00015.1, 2011.

Schnell, J. L. and Prather, M. J.: Co-occurrence of extremes in surface ozone, particulate matter, and temperature over eastern North America, Proceedings of the National Academy of Sciences, 114, 2854–2859, https://doi.org/10.1073/pnas.1614453114, http://www.pnas.org/content/114/11/2854.abstract, 2017.

Seneviratne, S. I., Nicholls, N., Easterling, D., Goodess, C. M., Kanae, S., Kossin, J., Luo, Y., Marengo, J., McInnes, K., Rahimi, M., Reichstein, M., Sorteberg, A., Vera, C., Zhang, X., Rusticucci, M., Semenov, V., Alexander, L. V., Allen, S., Benito, G., Cavazos, T.,

Atmospheric
Chemistry
and Physics
Discussions

Clague, J., Conway, D., Della-Marta, P. M., Gerber, M., Gong, S., Goswami, B. N., Hemer, M., Huggel, C., van den Hurk, B., Kharin, V. V., Kitoh, A., Tank, A. M. K., Li, G., Mason, S., McGuire, W., van Oldenborgh, G. J., Orlowsky, B., Smith, S., Thiaw, W., Velegrakis, A.,
5   Yiou, P., Zhang, T., Zhou, T., and Zwiers, F. W.: Changes in Climate Extremes and their Impacts on the Natural Physical Environment, in: Managing the Risks of Extreme Events and Disasters to Advance Climate Change Adaptation: Special Report of the Intergovernmental Panel on Climate Change, edited by Field, C. B., Barros, V., Stocker, T. F., and Dahe, Q., pp. 109–230, Cambridge University Press, Cambridge, https://doi.org/10.1017/CBO9781139177245.006, 2012.

Shen, L., Mickley, L. J., and Gilleland, E.: Impact of increasing heat waves on U.S. ozone episodes in the 2050s: Results from a multimodel
10   analysis using extreme value theory, Geophysical Research Letters, 43, https://doi.org/10.1002/2016GL068432, 2016.

Steiner, A. L., Davis, A. J., Sillman, S., Owen, R. C., Michalak, A. M., and Fiore, A. M.: Observed suppression of ozone formation at extremely high temperatures due to chemical and biophysical feedbacks, Proceedings of the National Academy of Sciences of the United States of America (PNAS), 107, 19 685–19 690, https://doi.org/10.1073/pnas.1008336107, 2010.

Sun, W., Hess, P., and Liu, C.: The impact of meteorological persistence on the distribution and extremes of ozone, Geophysical Research
15   Letters, 44, 1545–1553, https://doi.org/10.1002/2016GL071731, http://dx.doi.org/10.1002/2016GL071731, 2016GL071731, 2017.

Tilmes, S., Lamarque, J.-F., Emmons, L. K., Kinnison, D. E., Marsh, D., Garcia, R. R., Smith, A. K., Neely, R. R., Conley, A., Vitt, F., Val Martin, M., Tanimoto, H., Simpson, I., Blake, D. R., and Blake, N.: Representation of the Community Earth System Model (CESM1) CAM4-chem within the Chemistry-Climate Model Initiative (CCMI), Geoscientific Model Development, 9, 1853–1890, https://doi.org/10.5194/gmd-9-1853-2016, http://www.geosci-model-dev.net/9/1853/2016/, 2016.

20   Titchner, H. A. and Rayner, N. A.: The Met Office Hadley Centre sea ice and sea surface temperature data set, version 2: 1. Sea ice concentrations, Journal of Geophysical Research: Atmospheres, 119, 2864–2889, https://doi.org/10.1002/2013JD020316, http://dx.doi.org/10.1002/2013JD020316, 2013JD020316, 2014.

Weaver, C. P., Cooter, E., Gilliam, R., Gilliland, A., Grambsch, A., Grano, D., Hemming, B., Hunt, S. W., Nolte, C., Winner, D. A., Liang, X.-Z., Zhu, J., Caughey, M., Kunkel, K., Lin, J.-T., Tao, Z., Williams, A., Wuebbles, D. J., Adams, P. J., Dawson, J. P., Amar, P., He, S.,
25   Avise, J., Chen, J., Cohen, R. C., Goldstein, A. H., Harley, R. A., Steiner, A. L., Tonse, S., Guenther, A., Lamarque, J.-F., Wiedinmyer, C., Gustafson, W. I., Leung, L. R., Hogrefe, C., Huang, H.-C., Jacob, D. J., Mickley, L. J., Wu, S., Kinney, P. L., Lamb, B., Larkin, N. K., McKenzie, D., Liao, K.-J., Manomaiphiboon, K., Russell, A. G., Tagaris, E., Lynn, B. H., Mass, C., Salathé, E., O'neill, S. M., Pandis, S. N., Racherla, P. N., Rosenzweig, C., and Woo, J.-H.: A Preliminary Synthesis of Modeled Climate Change Impacts on U.S. Regional Ozone Concentrations, Bulletin of the American Meteorological Society, 90, 1843–1863, https://doi.org/10.1175/2009BAMS2568.1,
30   https://doi.org/10.1175/2009BAMS2568.1, 2009.

Wilson, A., Rappold, A. G., Neas, L. M., and Reich, B. J.: Modeling the effect of temperature on ozone-related mortality, The Annals of Applied Statistics, 8, 1728–1749, https://doi.org/10.1214/14-AOAS754, 2014.

Wu, S., Mickley, L., Jacob, D., Rind, D., and Streets, D.: Effects of 2000-2050 changes in climate and emissions on global tropospheric ozone and the policy-relevant background surface ozone in the United States, Journal of Geophysical Research: Atmospheres, 113, n/a–
35   n/a, https://doi.org/10.1029/2007JD009639, http://dx.doi.org/10.1029/2007JD009639, d18312, 2008.

Zhang, H., Wang, Y., Park, T.-W., and Deng, Y.: Quantifying the relationship between extreme air pollution events and extreme weather events, Atmospheric Research, 188, 64 – 79, https://doi.org/http://dx.doi.org/10.1016/j.atmosres.2016.11.010, http://www.sciencedirect.com/science/article/pii/S0169809516306093, 2017.

575 Zhu, J. and Liang, X.-Z.: Impacts of the Bermuda High on Regional Climate and Ozone over the United States, Journal of Climate, 26, 1018–1032, https://doi.org/10.1175/JCLI-D-12-00168.1, https://doi.org/10.1175/JCLI-D-12-00168.1, 2013.

Atmospheric
Chemistry
and Physics
Discussions

Open Access

EGU

Table 1. Details and descriptions for each model.

Simulation (Years)	GHG[1] forcing	Emissions	SST[2] and sea ice	Meteorology
REFC1SD[3] (1992-2010)	CMIP5[4] (updated until 2010)	Anthropogenic and biomass burning emission: MACCity[5] Biogenic emissions: MEGAN2[6]	HadISST2[7]	MERRA[8]
GCM2000 (2006-2025)	CO_2 = 369 ppm. Other GHG from REFC1SD.	Anthropogenic and biomass burning from AR5[9]. Biogenic emissions: Monthly values from MEGAN2 for 2000	Online[10]	Online[10]
GCM2100 (2106-2125)	CO_2 = 669 ppm. Other GHG as in GCM2000.	GCM2000	Online[10]	Online[10]

[1] Greenhouse gas. [2] Sea surface temperature. [3] REFC1SD model. [4] Coupled model intercomparison project. [5] Granier et al. (2011). [6] Guenther et al. (2012). [7] Hadley Center Sea Ice and Sea surface temperature data set (Titchner and Rayner (2014)). [8] Modern era retrospective-analysis for research and applications (Rienecker et al. (2011)). [9] Assessment report 5 (Eyring et al. (2013)). [10] Tilmes et al. (2016).

Atmospheric
Chemistry
and Physics
Discussions

Open Access

EGU

Table 2. [Rescaled Data] Ozone averages (ppb) and temperature averages (°C) in different regions over the U.S. from CASTNET data and corresponding grid points from different simulations. The averages are calculated from MDA8 (for ozone) and daily maximum (for temperature). Standard deviations (sd) are calculated between the stations in each region. The averages of ozone and temperature from each region are reported in italics (including all continental grid points in each box in Fig. 2a). The italics under 'All' are averages of all points over the continental US.

Region	CASTNET		REFC1SD		GCM 2000		GCM 2100	
	Ozone (sd)	Temp (sd)	Ozone (sd)	Temp (sd)	Ozone (sd)	Temp (sd)	Ozone (sd)	Temp (sd)
Northeast	45.46	23.01	59.48	19.81	66.46	23.39	71.03	25.98
	(9.9)	(1.8)	(7.59)	(1.4)	(11.08)	(1.53)	(11.06)	(1.33)
	60.33	*20.27*	*67.48*	*23.11*	*72.08*	*25.75*		
Southeast	52.71	25.38	62.31	24.86	72.62	27.46	75.34	29.36
	(4.99)	(3.17)	(8.63)	(1.77)	(9.81)	(0.9)	(10.68)	(0.59)
	61.56	*24.90*	*72.27*	*27.59*	*74.88*	*29.5*		
Midwest	44.67	25.91	65.1	23.68	77.59	27.67	80.95	30.16
	(8.22)	(3.93)	(8.11)	(1.53)	(7.8)	(1.42)	(7.24)	(1.35)
	64.63	*23.61*	*77.92*	*27.50*	*81.67*	*29.97*		
West	51.29	22.27	60.47	21.81	66.15	26.62	67.1	29.12
	(7.52)	(4.37)	(9.46)	(5.07)	(6.92)	(4.35)	(6.47)	(3.81)
	61.39	*22.30*	*67.61*	*26.59*	*68.68*	*29.19*		
All	49.72	24.25	61.6	22.9	70.45	26.34	73.33	28.6
	(7.63)	(3.39)	(8.16)	(3.27)	(9.75)	(2.67)	(10.14)	(2.33)
	54.28	*22.76*	*61.65*	*26.16*	*63.72*	*28.59*		

Atmospheric
Chemistry
and Physics
Discussions

Open Access

EGU

Table 3. [Rescaled Data] Twenty-year return levels ozone (ppb) and temperature ($^\circ C$) (first and third columns). Twenty-year return levels ozone and temperature minus their averages (second and fourth columns). The models are sampled only at the CASTNET stations.

Model	Region	Ozone [ppb]		Temperature [$^\circ C$]	
		20-year return	Minus mean	20-year return	Minus mean
CASTNET	Northeast	102.06	56.63	33.7	10.72
	Southeast	99.04	46.49	32.9	7.55
	Midwest	90	45.36	34.46	8.55
	West	78.61	27.35	32.42	10.2
	All	94.59	44.96	33.18	8.96
REFC1SD	Northeast	103.49	44.01	27.38	7.57
	Southeast	100.56	38.25	30.52	5.66
	Midwest	107.57	42.47	31.34	7.66
	West	88.07	27.59	29.36	7.55
	All	99.6	38.01	29.63	6.73
GCM 2000	Northeast	100.92	34.45	31.66	8.27
	Southeast	107.23	34.61	33.39	5.93
	Midwest	110.19	32.6	36.19	8.52
	West	85.84	19.68	32.56	5.94
	All	101.79	31.35	33.15	6.81
GCM 2100	Northeast	105.25	34.22	33.85	7.87
	Southeast	105.61	30.28	35.65	6.28
	Midwest	114.17	33.22	40.01	9.86
	West	87.6	20.5	36.05	6.94
	All	102.95	29.62	35.82	7.22